Eur. Phys. J. C (2024) 84:291
https://doi.org/10.1140/epjc/s10052-024-12605-z

THE EUROPEAN PHYSICAL JOURNAL C

Regular Article - Theoretical Physics

Collisions and dynamics of particles with magnetic dipole moment and electric charge near magnetized rotating Kerr black holes

Shokhzod Jumaniyozov[1,2,a], **Saeed Ullah Khan**[3,4,b], **Javlon Rayimbaev**[5,6,7,c], **Ahmadjon Abdujabbarov**[1,8,d], **Bobomurat Ahmedov**[1,9,e]

[1] Ulugh Beg Astronomical Institute, Astronomy Str. 33, 100052 Tashkent, Uzbekistan
[2] Institute of Nuclear Physics, Ulugbek 1, 100214 Tashkent, Uzbekistan
[3] College of Mathematics and Statistics, Shenzhen University, Shenzhen 518060, China
[4] College of Physics and Optoelectronic Engineering, Shenzhen University, Shenzhen 518060, China
[5] School of Mathematics and Natural Sciences, New Uzbekistan University, Movarounnahr St. 1, 100007 Tashkent, Uzbekistan
[6] Faculty of Computer Engineering, University of Tashkent for Applied Sciences, Gavhar Str. 1, 700127 Tashkent, Uzbekistan
[7] Institute of Fundamental and Applied Research, National Research University TIIAME, Kori Niyoziy 39, 100000 Tashkent, Uzbekistan
[8] Tashkent State Technical University, 100095 Tashkent, Uzbekistan
[9] Institute of Theoretical Physics, National University of Uzbekistan, 100174 Tashkent, Uzbekistan

Received: 7 January 2024 / Accepted: 21 February 2024 / Published online: 20 March 2024

Abstract Analysis of test magnetized and charged particles around black holes immersed in external magnetic fields may help to explain the observed astrophysical phenomena related to black holes, such as the acceleration of particles up to high energies. In this sense, we studied the circular motion of test-charged particles with magnetic dipole orbiting around magnetized rotating Kerr black holes. First, we derive the effective potential for the circular motion of such particles, including interactions between the external magnetic field and the electric charge, and the magnetic interaction between the magnetic dipole. In addition, we analyze the angular momentum and energy of particles corresponding to circular orbits. The effects of magnetic interaction and coupling parameters on the position of innermost stable circular orbits (ISCOs), the energy and angular momentum of the particles at ISCO, and the energy efficiency from the Novikov-Thorne accretion disc have been investigated. We also find cases of degeneracy between magnetic dipole interaction and magnetic coupling parameters, giving the same ISCO radius. Finally, we studied various cases of collisions of neutral, magnetized, and electrically charged particles near rotating Kerr black holes in the presence of external magnetic fields. The critical angular momentum of spinning charged particles is found in which the particles can collide. We also analyze the effects of both magnetic interactions on the center-of-mass energy of the colliding particles.

1 Introduction

Testing gravity theories using observational data is an important task of relativistic astrophysics because gravity theories are a key concept in understanding the formation and evolution of the Universe, as well as the behavior of astronomical objects such as stars and galaxies, as well as the physics of gravitational compact relativistic objects: black holes and neutron stars.

One of the most important and well-tested gravity theories is general relativity, describing gravity as a curvature of spacetime, which was developed by Albert Einstein in the early 20th century. It has been incredibly successful in explaining a wide range of astronomical phenomena, such as the bending of light around massive objects [1,2], the precession of Mercury's orbit, and the existence of black holes. However, there are still a few open fundamental problems of current relativistic astrophysics related to the nature of dark matter and dark energy. On the other hand, astrophysical magnetic fields are also important for understanding the Universe. The magnetars, pulsars, white dwarfs, stars, and accretion disks of black holes may play the role of the source of a strong magnetic field. Thus, the effect of gravity is important in the study of powerful magnetic field sources.

[a] e-mail: jumaniyozovshohzod@gmail.com
[b] e-mail: saeedkhan.u@gmail.com (corresponding author)
[c] e-mail: javlon@astrin.uz
[d] e-mail: ahmadjon@astrin.uz
[e] e-mail: ahmedov@astrin.uz

In astrophysics, the magnetic fields play a vital role in explaining many astrophysical processes, such as the formation of stars and planets, the acceleration of cosmic rays, and the ejection of jets from black holes. Magnetic fields can also confine and heat plasma, the fourth state of matter that makes up most of the visible Universe.

The solutions of the Maxwell equations around both Schwarzschild and Kerr black holes immersed in an external asymptotically uniform magnetic field were first obtained by Wald in 1974 [3]. Petterson [4] proposed the dipole magnetic field, which may be formed using the circular current loops surrounding the black hole. The split-monopole magnetic field approximation, along with the parabolic field, has been explored in [5]. It should be noted that parabolic fields are typically the consequences of numerical modeling of toroidal configurations considered within the context of general relativistic magnetohydrodynamics [6].

In astrophysics, it is important to consider magnetic field effects on particle dynamics in the black holes accretion discs. However, astrophysical magnetic fields around black holes are difficult to observe directly. Thus, their effects can be observed in various ways, such as the emission of polarized light and the acceleration of charged and magnetized particles. Besides, the astrophysical compact entities' magnetic fields are responsible for witnessing high-energy processes in their vicinity. This may be utilized to validate theories of gravity in an intense field environment by examining the dynamics of charged and magnetized particles. In this sense, gravity theories and astrophysical magnetic fields are important in understanding the Universe.

In past years, using the Walds approach, several studies have been performed through the dynamics and radiation of charged and magnetized particles [7–15]. Recently, Khan and Chen [16], by studying the dynamics of charged particles in the black hole split-monopole magnetosphere, discovered that the positive magnetic field boosts the stability of circular orbits. The motion of magnetized particles near black holes in the existence of an external magnetic field has been studied in [17–23].

Observations of electromagnetic fields around black holes in different bands have yielded valuable information about the dynamical processes around Sgr A*. The evaluated value of the magnetic field strength from the vicinity of Sgr A* to the innermost edge of its accretion is approximately 5–100 G [24,25], and its estimated value around the orbit of PSR 1745–2900 is about few mG [26]. Another important issue is related to the magnetic field configuration. Although there exist numerous theoretical studies on astrophysical events in the vicinity of the supermassive black hole Sgr A*, the magnetic field configuration in the close environment of the black hole is still not defined [27].

Particle collisions around a revolving and charged black hole's horizon is an essential and engaging process that can end up with high-energy emissions. To date, various physical mechanisms have been presented as black hole energy extraction techniques. Roger Penrose [28] was the pioneer in describing an easy mechanism for extracting energy from black holes. Piran et al. [29,30] have investigated such mechanisms associated with the Penrose phenomenon. Banados, Silk, and West (BSW) [31] observed that collisions could yield high center-of-mass energy particles for an excessively spinning black hole. Such energy could be greater than Planckian energy in an idealistic set-up; therefore, black holes may be considered an ultra-high energy collider. By studying the charged Gauss–Bonnet-AdS black hole, Zahid et al. predicted that whenever a pair of neutral electrical test particles collide near the horizon of a black hole, it may act as a particle accelerator with arbitrarily enormous center-of-mass energy [32,33]. Investigating this problem has attracted a great deal of attention in recent years [34–39].

Several mechanisms exist that minimize the possibility of large collision energy [40,41]. In the case of fast-rotating black holes, the center-of-mass energy will be endlessly large. A little breach of the extremity criterion, which is virtually unavoidable in astrophysical applications, greatly reduces this impact. Particle trajectories require considerable fine-tuning, even in an idealized spinning situation. This mechanism is also heavily influenced by gravitational radiation [42].

In our previous works [43,44], we have studied electrically charged particles with magnetic dipole moment in spacetime around Schwarzschild and Schwarzschild-MOG black holes located in external asymptotically uniform magnetic fields. In this work, we aim to extend the studies into magnetized rotating Kerr black hole spacetime.

Here, we plan to study the dynamics of magnetized and electrically charged particles around Kerr black holes in the presence of an external magnetic field. The paper is organized as follows: we briefly review magnetized Kerr black holes as a solution of the Maxwell equations in Sect. 2. We explore the equation of motion of charged/magnetized particles around Kerr black holes in the presence of magnetic fields in Sect. 3. Section 4 is devoted to the analysis of particle collisions near rotating magnetized black holes. We summarize the results obtained in Sect. 5. Throughout the paper, we use geometrized units $c = G = 1$ and run Latin indexes from 0 to 3 and Greek indexes from 1 to 3.

2 Magnetized Kerr black holes

The spacetime geometry of the rotating Kerr black hole with the total mass M and rotating parameter a can be described by the following line element

$$ds^2 = g_{tt}dt^2 + 2g_{t\phi}dtd\phi + g_{rr}dr^2 + g_{\theta\theta}d\theta^2 + g_{\phi\phi}d\phi^2, \quad (1)$$

where the nonzero components of the metric tensor are defined as

$$g_{tt} = -\left(1 - \frac{2Mr}{\Sigma}\right), \quad g_{rr} = \frac{\Sigma}{\Delta}, \quad g_{\theta\theta} = \Sigma,$$
$$g_{\phi\phi} = \left(r^2 + a^2 + \frac{2Mr}{\Sigma}a^2 \sin^2\theta\right)\sin^2\theta,$$
$$g_{t\phi} = -\frac{2Mra}{\Sigma}\sin^2\theta$$

with $\Sigma = r^2 + a^2\cos^2\theta, \quad \Delta = r^2 + a^2 - 2Mr.$

One may consider the test field around the rotating black hole. Magnetic fields around black holes satisfying the condition $B \ll 10^{19}(M_\odot/M)$G are considered to be weak, which cannot contribute to the space-time curvature of the black hole [45].

The structure of the external magnetic field near the black hole horizon could be highly complicated. Near the structure's rotation axis, where jets might exist, a parabolic magnetic field, irrespective of the magnetic field's original layout, is correlated. As a result, it may be appropriate to retain the asymptotically uniform magnetic field suggested by Wald [3] and used in numerous significant investigations of cosmic problems as the initial fundamental estimate. To maintain the space-time configuration's symmetry, the lines of magnetic fields must be assumed to be oriented alongside the rotational axis.

With the assumption of an asymptotically uniform magnetic field of intensity B and lines directed alongside the z-axis in our model of the magnetosphere, the corresponding non-vanishing elements of the electromagnetic potential four-vector A_{mu} can be expressed as

$$A^\mu = \frac{B}{2}\left(\xi^\mu_{(\phi)} + 2a\xi^\mu_{(t)}\right) - \frac{Q}{2M}\xi^\mu_{(t)}. \tag{2}$$

In the expressions, (2) Q represents the induced electric charge of the black hole spacetime. In the case of chargeless black holes, the parameter $Q = 0$ and the maximum produced black hole charge caused by the black hole spin and the magnetic field. This so-called Wald charge is defined as $Q_W = 2aB$, which results in a potential drop between the black hole center and infinity. Authors of Ref. [46] have estimated that the Wald charge is much lower than the critical charge, which may affect spacetime. Therefore, in our analyses, we consider the chargeless rotating black hole by setting $Q = 0$ as

$$A_t = \frac{B}{2}\left(g_{t\phi} + 2ag_{tt}\right), \quad A_\phi = \frac{B}{2}\left(g_{\phi\phi} + 2ag_{t\phi}\right). \tag{3}$$

3 Equations of motion of magnetized particles with nonzero electric charge near magnetized Kerr black holes

The Hamilton-Jacobi method is a useful tool to determine the equations of charged and magnetized particles' motion around a magnetized Kerr black hole in the following generalized form:

$$g^{\mu\nu}\left(\frac{\partial\mathcal{S}}{\partial x^\mu} + eA_\mu\right)\left(\frac{\partial\mathcal{S}}{\partial x^\nu} + eA_\nu\right) = -\Big(m + U\Big)^2, \tag{4}$$

where, the term $2U = D^{\mu\nu}F_{\mu\nu}$ is responsible for the interaction between the magnetic dipole and the external magnetic field, $D^{\mu\nu}$ and $F_{\mu\nu}$ are the polarization tensors and the electromagnetic field, respectively. The expression for the tensor $D^{\mu\nu} = \eta^{\alpha\beta\sigma\nu}u_\sigma\mu_\nu$ satisfies the condition $D^{\alpha\beta}u_\beta = 0$, where μ^ν refers to the vector of four dipole moment and u^ν is the four-velocity of the particle.

The expression of the electromagnetic field tensor $F_{\alpha\beta} = 2u_{[\alpha}E_{\beta]} + \eta_{\alpha\beta\sigma\gamma}u^\sigma B^\gamma$ helps to find non-zero components of the external magnetic field as

$$B^\alpha = \frac{1}{2}\eta^{\alpha\beta\sigma\mu}F_{\beta\sigma}u_\mu \tag{5}$$

where $\eta^{\alpha\beta\sigma\mu} = \sqrt{-g}\epsilon^{\alpha\beta\sigma\mu}$ with the Levi–Civita symbol $\epsilon^{\alpha\beta\sigma\mu}$ and the metric determinant $g = det(g_{\mu\nu})$.

In our further analysis, we assume the direction of the dipole moment is perpendicular to the equatorial plane and has the following components: $\mu^{\hat{i}} = (0, \mu^{\hat{\theta}}, 0)$, which is always parallel to the magnetic field lines and perpendicular to the equatorial plane. Thus, the interaction term U for the zero angular momentum observer (ZAMO) has the form $U = 2\mu^{\hat{\theta}}B_{\hat{\theta}}$, where the magnetic field [46]

$$B^{\hat{\theta}} = -\frac{B_0 r\sin^2\theta\sqrt{\Delta}}{\Sigma^2 A} \times\left\{\left[\Delta - \left(1 - \frac{M}{r}\right)\Sigma - a^2\sin^2\theta\right] \times a^2(1 + \cos^2\theta) - \Sigma^2\right\}. \tag{6}$$

Finally, at the equatorial plane, the interaction term takes the form, $U = 2\mu B_0 F(r)$, where

$$F(r) = \frac{a^2M - r^3}{r(r^2 + a^2)}\sqrt{1 - \frac{2M}{r} + \frac{a^2}{r^2}}. \tag{7}$$

The integrals of motion for electrically charged particles with magnetic dipole moment can be found using the time translation and the rotational symmetry of the geometry can be determined by the following form Lagrangian [47, see

Eq.(7)]

$$\mathscr{L} = \frac{1}{2}\Big[(m+U)g_{\mu\nu}u^{\mu}u^{\nu} - kU\Big] + eA_{\mu}u^{\mu} \tag{8}$$

and the corresponding conserved quantities are the specific energy $\mathcal{E} = E/m$ of the moving particle and its angular momentum $\mathcal{L} = L/m$. Consequently, we have

$$-\mathcal{E} = (1+\beta F(r))\left[g_{tt}\dot{t} + g_{t\phi}\dot{\phi}\right] + qA_t, \tag{9}$$

$$\mathcal{L} = (1+\beta F(r))\left[g_{\phi\phi}\dot{\phi} + g_{t\phi}\dot{t}\right] + qA_{\phi}, \tag{10}$$

where $\mathcal{L} = L/m$ is the specific angular momentum of the particles and $\beta = \mu B/(2m)$ is the magnetic coupling parameter corresponding to the magnetic interaction between the magnetic dipole moment of the particles and $q = e/m$ is the charge to mass relation.

The dynamics of electrically charged particles with magnetic dipole moment orbiting the magnetized Kerr black hole at the equatorial plane (i.e., $\theta = \pi/2$ and $u^{\theta} = \dot{\theta} = 0$) will be described by the following action:

$$\mathcal{S} = -Et + L\phi + \mathcal{S}_r. \tag{11}$$

Then, we can derive the equation for the radial coordinate using the Hamilton–Jacobi equation (4), taking into account the Eqs. (9) and (10). With this in mind, we can write the variables in a separate form in the Hamilton-Jacobi equation. The radial motion of the particle can then be defined by

$$\begin{aligned} g_{rr}\dot{r}^2 &= \alpha\mathcal{E}^2 + 2\delta\mathcal{E} + \gamma \\ &= \left[\mathcal{E} - V_{\rm eff}^{+}(r)\right]\left[\mathcal{E} - V_{\rm eff}^{-}(r)\right] \end{aligned} \tag{12}$$

where $\alpha = -g^{tt}$, $\delta = g^{t\phi}\left(\mathcal{L} + qA_{\phi}\right) + g^{tt}qA_t$ with

$$\begin{aligned} \gamma = {} & g^{tt}q^2A_t^2 + g^{\phi\phi}\left(\mathcal{L} + qA_{\phi}\right)^2 + 2g^{t\phi}qA_t\left(\mathcal{L} + qA_{\phi}\right) \\ & + (1+\beta F(r))^2 \end{aligned}$$

and $V_{\rm eff}(r)$ for the circular motion ($\dot{r} = 0$) of charged magnetized particles has the form

$$V_{\rm eff}^{\pm} = \frac{-\delta \pm \sqrt{\delta^2 - 4\alpha\gamma}}{2\alpha}. \tag{13}$$

In this study, we consider the positive root of the effective potential, $V_{\rm eff}^{+}$, as it corresponds to the so-called positive root states with four-velocity oriented to future and positive energy relative to local observers (see, e.g., [48,49]).

In Fig. 1, we present the radial dependency of the effective potential for different values of the black hole spin a, ω_B, and β. It is observed that the presence of $\omega_B > 0$ ($\omega_B < 0$) causes an increase (decrease) in the effective potential. While in the presence of the magnetic field and β, the effective potential increases, particularly β greatly influenced it along the radial distance r. Our examination reflects that particles with magnetic dipole moment and electric charge have the highest unstable circular orbits in fast-rotating magnetized Kerr black holes with a compare to slow-rotating ones.

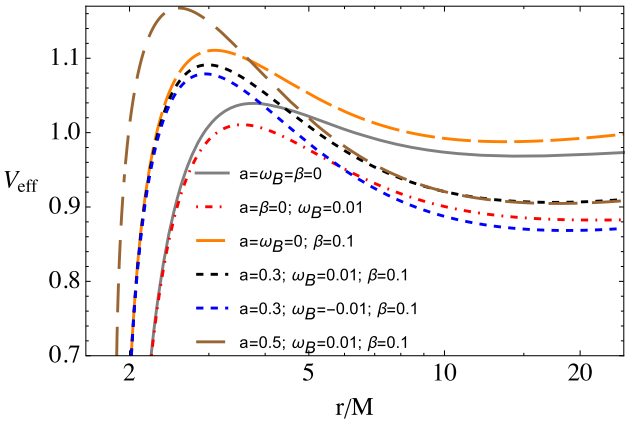

Fig. 1 Radial profiles of $V_{\rm eff}$ for different values of β, a and $\omega_B = qB/2m$ parameters

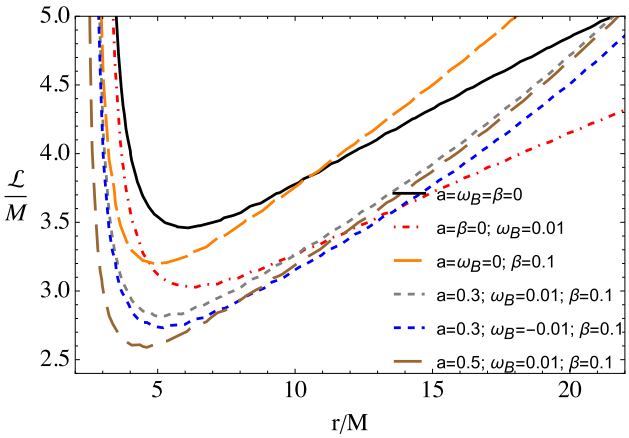

Fig. 2 The angular momentum of magnetized test-charged particles orbiting magnetized Kerr black holes at different values of the parameters β, a and ω_B

3.1 Circular orbits

This subsection aims to explore the circular motion of the magnetized and charged particles around magnetized Kerr black holes. In general, no radial forces/motion along the circular orbits or the present forces counterbalance each other at the appropriate angular momentum values of the particles.

The orbit circularity of magnetized test-charged particles orbiting around magnetized black holes may be investigated assuming the limitations $V_{\rm eff} = \mathcal{E}$ and $V'_{\rm eff} = 0$, wherein the prime represents the partial derivative over r. As a result of these conditions, one can determine the angular momentum and energy of a particle in circular orbits.

Figure 2, depicts the graphical illustration of the angular momentum of the magnetized and charged particles for the different parametric values of ω_B, a, and β. We find out that

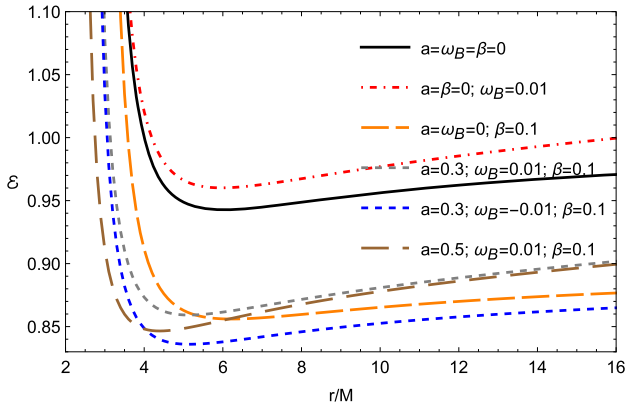

Fig. 3 Graphical description of the Energy $\mathcal{E}$ of the magnetized test-charged particles orbiting magnetized Kerr black holes at different values of the parameters β, a and ω_B

magnetic fields contribute to the minima of angular momentum in both positive and negative cases of the Larmor frequency parameter ω_B. One can also note that $\omega_B < 0$ has more impact on the minima of angular momentum in comparison with $\omega_B > 0$. Moreover, we found that black hole spin a significantly contributes to the minima of angular momentum. Surprisingly, the magnetized Kerr black holes have the smallest minima as compared to the Schwarzschild and Schwarzschild-MOG black holes (see Fig.2 in Refs. [43,44]).

In Fig. 3, we have graphically interpreted the behavior of magnetized test-charged particle's energy orbiting magnetized Kerr black holes at different values of the parameters β, a and ω_B. Our investigation revealed that the energy behaves quite similarly to the angular momentum under the impact of these parameters. In addition, one should note that here a also influences the energy minima. Our results showed that the magnetic field considerably decreases the energy and angular momentum of the magnetized test-charged particles orbiting magnetized Kerr black holes. Also, one noticed that the magnetized Kerr black holes have the least minima in comparison with the Schwarzschild and Schwarzschild-MOG black holes (see our previous papers [43,44]). In addition, the $\omega_B < 0$ further enhances the minima in the orbital energy of the particles with magnetic dipole and electric charge.

3.2 Innermost stable circular orbits

The solution of $V'_{\rm eff} = 0$ for r helps locate the position of the orbits, where the effective potential has its maximum values. The minima of effective potential corresponds to the stability of circular orbits. In other words, at $V''_{\rm eff}(r) < 0$, the circular orbits become unstable, while all circular stable orbits fulfill the prerequisite of $\partial_{rr} V_{\rm eff}(r_{\rm ISCO}) > 0$. On the contrary, ISCO complies with the requirements of $\partial_{rr} V_{\rm eff}(r_{\rm ISCO}) = 0$.

Figure 4 demonstrates the graphical representation of ISCO radius against the Larmor frequency β (left panel) and

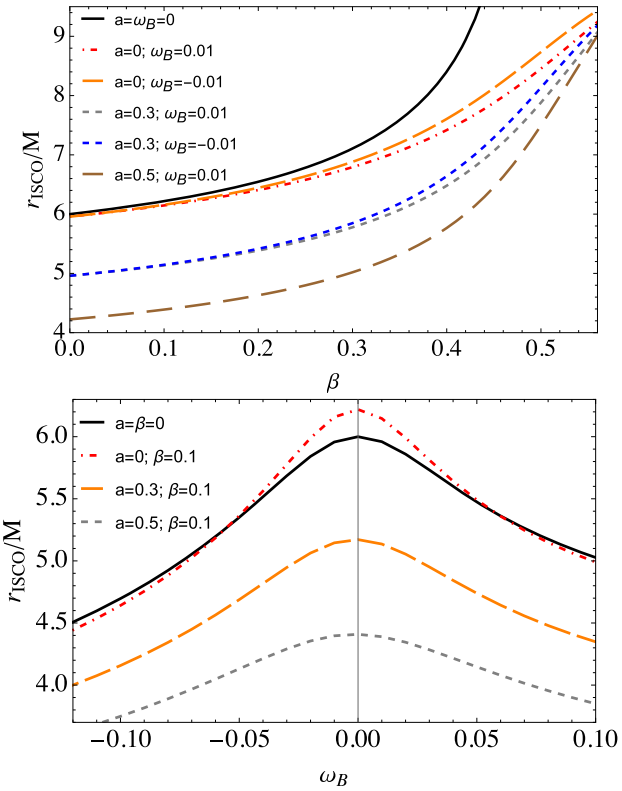

Fig. 4 Visual depiction of the ISCO radius vs β and ω_B, at various discrete values of black hole spin a and ω_B

ω_B (right panel) for different values of the black hole spin. Our analysis reveals that the magnetic coupling parameter β contributes to the ISCO radius. From Fig. 4, it can also be observed that the black hole spin a and the Larmor frequency $|\omega_B|$ result in decreasing the ISCO radius. Moreover, the Schwarzschild-MOG black holes (see Fig. 5 in [43]) have the highest ISCO as compared to the Schwarzschild black holes (see Fig. 3 in [44]) and magnetized Kerr black holes. Besides, we also observe that at a particular value of ω_B, the ISCO radius remains unaffected by the magnetic coupling parameter β, providing the same values of ISCO radius (see red-dot dashed and black solid lines).

Figure 4 also shows the dependency of the ISCO radius along the magnetic coupling parameter β. We observed that the ISCO radius significantly increases with the increase of β in the case of $\omega_B = 0$, while it decreases along the magnetic coupling β in the presence of Larmor frequency ($\omega_B \neq 0$). Also now, here we are interested in degeneracy values between Larmor frequency ω_B and magnetic interaction parameters providing the same ISCO radius.

In Fig. 5, we have plotted the relationships between ω_B and β for the same values of ISCO radius. The graphical interpretation shows the relationships as contours: at larger magnetic field values, the contours became smaller. Also, the contour enlarges with increasing black hole spin.

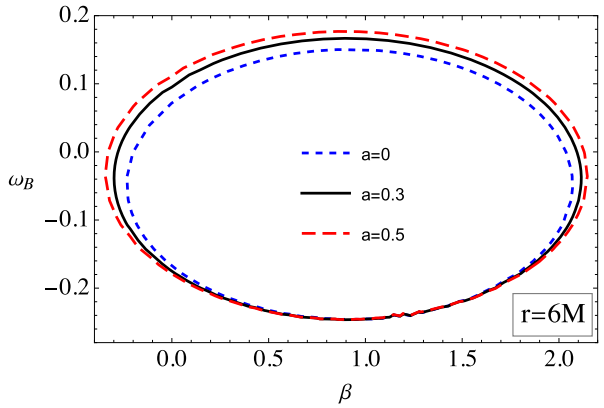

Fig. 5 Visual depiction of ω_B vs β at various values of ISCO radius for the case of $r = 6M$

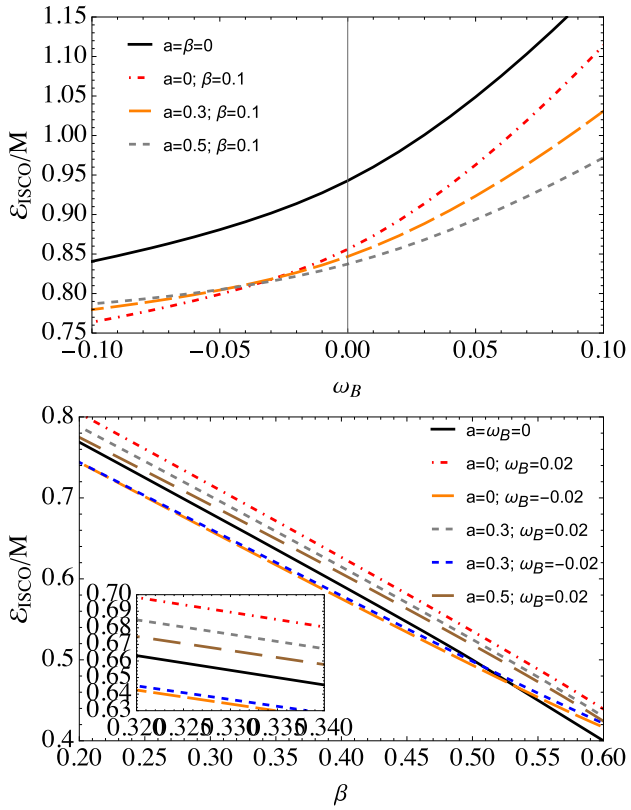

Fig. 6 Graphical illustration of the energy of particles at their ISCO at various values of β and ω_B

3.3 The ISCO energy of particles

In the following subsection, we examine the impact of various values of the parameters a, β, and ω on the energy of the test particle in its ISCO.

Figure 6 shows dependencies of the energy of charged magnetized particles orbiting magnetized Kerr black holes at the ISCO along the parameters ω_B (upper row) and β (lower row). It can be seen that increases of ω_B cause an increase in the energy at ISCO $\mathcal{E}_{ISCO}$. Moreover, both the black hole spin and magnetic interaction parameters have a significant impact on the particle's energy at ISCO and considerably decrease it. Also, one can observe from the top panel that at a certain negative value of ω_B, $\mathcal{E}_{ISCO}$ take the same value.

3.4 The ISCO angular momentum

Here, we will study the effects of the magnetic interaction and spin parameters on the angular momentum of charged magnetized particles at their ISCOs.

In Fig. 7, we have plotted the behavior of the specific angular momentum of charged magnetized particles vs. ω_B and β in the top and bottom rows, respectively. From where one can observe that the black hole spin a diminishes the ISCO's angular momentum ($\mathcal{L}_{ISCO}$). While the Larmor frequency ω_B increases the angular momentum, whereas β causes a decrease in it. Furthermore, the negative value of ω_B decreases the angular momentum of the particles at ISCO compared to its positive value. Moreover, the Schwarzschild black hole has greater angular momentum at the ISCO as compared to the magnetized Kerr black holes, and it further decreases as the black hole rotates faster.

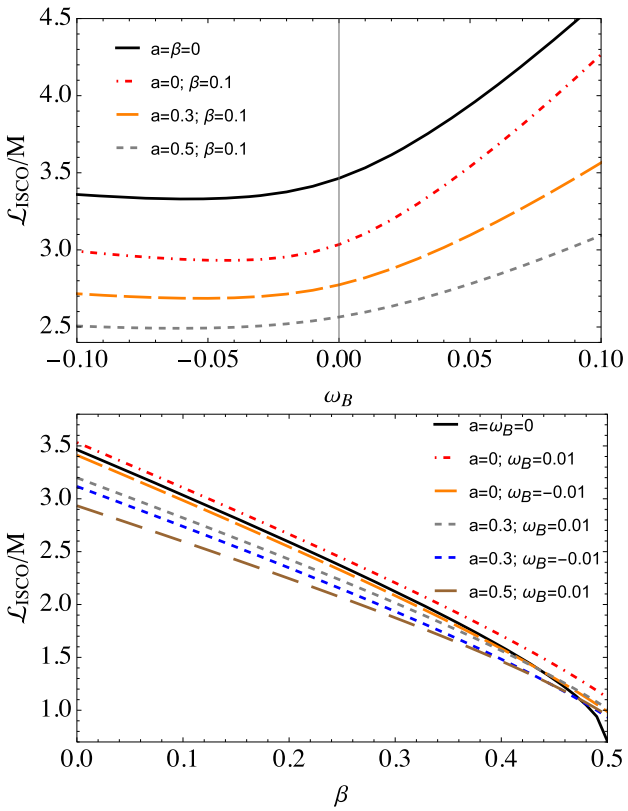

Fig. 7 Graphical illustration of the angular momentum of particles at ISCO at various β, ω_B, and a parameter values

3.5 Energy efficiency

Another intriguing scenario emerges when examining a test particle within a Keplerian accretion disk as it descends towards the central black hole, releasing energy in the form of electromagnetic and/or gravitational radiation. The amount of radiated energy is dictated by the contrast between the particle's rest energy, as observed locally, and its energy at the ISCO, which serves as a reflection of the spacetime characteristics. Consequently, one can compute the energy efficiency of the accretion disk using the expression provided by Novikov in 1973 [50].

The ISCO significance in the vicinity of black holes is linked to the inner boundary of an accretion disk. Surprisingly, as testing particles plunge into the center of the black hole within the Keplerian accretion disk, they extract a certain amount of energy that might be converted to electromagnetic and gravitational radiation upon limitations. The amount of released energy via radiations is often calculated as the difference between the particle's rest energy (as determined by an appropriate viewer) and the particle's ISCO energy ($\mathcal{E}_{\rm ISCO}$) [50]. Indeed, the bolometric luminosity of the brightness emanating from the accretion disk is directly linked to the energy efficiency of the central black hole, as expressed by the equation $\eta = L_{\rm bol}/(\dot{M}c^2)$, where $\dot{M}$ signifies the accretion rate [51].

Here, we also study the efficiency of released energy at various parametric values of the magnetic coupling and magnetic interaction between the magnetic field and the particles' electric charge, as well as the magnetic dipole moment. As a result, the efficiency of the accretion disk's released energy can mathematically be represented as [50]

$$\eta = 1 - \mathcal{E}|_{r_{\rm ISCO}}. \tag{14}$$

In Fig. 8, we have plotted the behavior of the energy extraction efficiency along ω_B and β in the upper and lower rows, respectively. Our graphical analysis demonstrated that black hole spin a contributes to the process of energy extraction. In addition, the parameters ω_B and β considerably influence the process of energy extraction. One can extract much more energy in the case of $\beta \neq 0$ compared to $\beta = 0$, whereas $\omega_B < 0$ contributes to the energy extraction while $\omega_B > 0$ decreases it. Moreover, our analysis shows that more energy can be extracted from rotating black holes in comparison with static ones. Also, it is observed from the top panel that at a certain negative value of ω_B, the energy efficiency at different a takes the same value for $\beta = 0.1$.

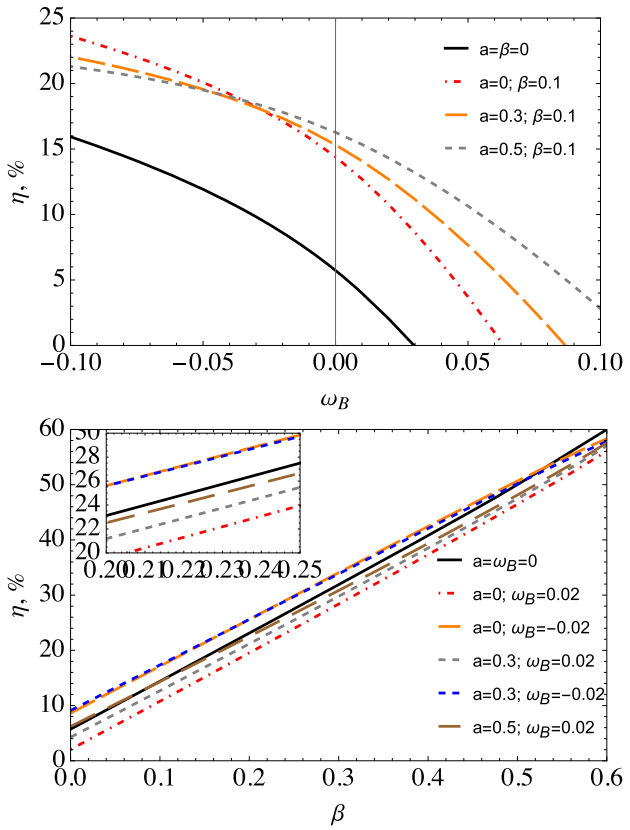

Fig. 8 Graphical behavior of the energy efficiency as a function of ω_B (top panel) and β (bottom panel)

4 Particle collisions near magnetized Kerr black holes

The collisional process near black holes remains a significant and intriguing general relativity topic. The extraction of energy may take place from a black hole throughout the collision process. A variety of methodologies may be employed to investigate the process of extracting energy from a spinning-charged black hole. Determining the entire amount of energy extracted via various methods taking place around black holes could clarify the reason why the intensity of AGN is on a scale of 10^{45}erg/s, which might be driven by supermassive black holes.

Among others, Penrose [28] was the first who laid the foundation of an easy process according to which a particle entering the ergosphere of a spinning hole breaks down into a pair of particles: one of them crashes into the black hole while another travels to infinity with more energy compared to the original particle. The technique in question has recently been explored in various studies in the literature; for details, see [52–54]).

Banados–Silk–West (BSW) [55,56] investigated particle collisions around the horizons of black holes as an approach to extract energy, which was further explored in [56–71]. It is observed that the efficiency of energy extraction from the center black hole is proven to be greater through head-on collisions.

Here, we focus exploring the collisions of test electrically charged, magnetized, and neutral particles within the metric of magnetized rotating Kerr black holes. We use the generic equation presented in [55] for the center of mass energy $E_{\rm cm}$ of interacting particles.

$$\left(\frac{1}{\sqrt{-g_{tt}}}E_{\rm cm},0,0,0\right)=m_1u^{\mu}_{(1)}+m_2u^{\nu}_{(2)}, \tag{15}$$

where m_i and $u^{\mu}_{(i)}$, respectively stands mass of the ith particle ($i=1,2$) and corresponding four-velocity. Using the normalization conditions $g_{\mu\nu}u^{\mu}u^{\nu}=-1$, we can easily calculate the expression for $E_{\rm cm}$ as

$$\frac{E^2_{cm}}{m_1m_2}=\frac{m_1^2+m_2^2}{m_1m_2}-2g_{\mu\nu}u^{\mu}_1u^{\nu}_2. \tag{16}$$

We address straightforward situations by considering $m_1=m_2=m$ (masses) in our subsequent analysis.

4.1 Critical angular momentum of colliding particles

In practice, in the case of particle collisions, the center of mass energy remains maximal at close orbits near the event horizon. At the same time, the particle collision's axial velocity fulfills the requirements $\dot{r}^2\geq 0$ as a function of the angular momentum $\dot{r}^2(\mathcal{L})$ and the other parameters. The radial velocity and its first derivative with respect to r vanishes ($\dot{r}=0$, and $\partial_r(\dot{r}^2)=0$) once the angular momentum reaches its threshold values. However, the radial velocity diminishes as the angular momentum increases. the challenging system of equations can be solved numerically.

In Fig. 9, we have plotted the behavior of the critical values of angular momentum at various parametric values of β in $\omega_B=-0.01$ (top panel) and $\omega_B=0.01$ (bottom panel). From the graphical behavior, we observed that the difference between the angular momentum's critical values increases along the black hole's spin and becomes larger in the fast-spinning black holes. On the other hand, both the black hole spin and the magnetic coupling parameter β contribute to increasing in $\mathcal{L}_{\rfloor\nabla}$.

4.2 Center of mass energy of particles in different scenarios.

This portion looks at the collisions between electrically neutral, magnetized, and electrically charged particles having a dipole magnetic moment. Taking into account particles of identical masses, the center of mass energy provided in Eq. (16) has the following form:

$$\frac{E^2_{cm}}{m^2}=2\left(1-g_{\mu\nu}u^{\mu}_1u^{\nu}_2\right). \tag{17}$$

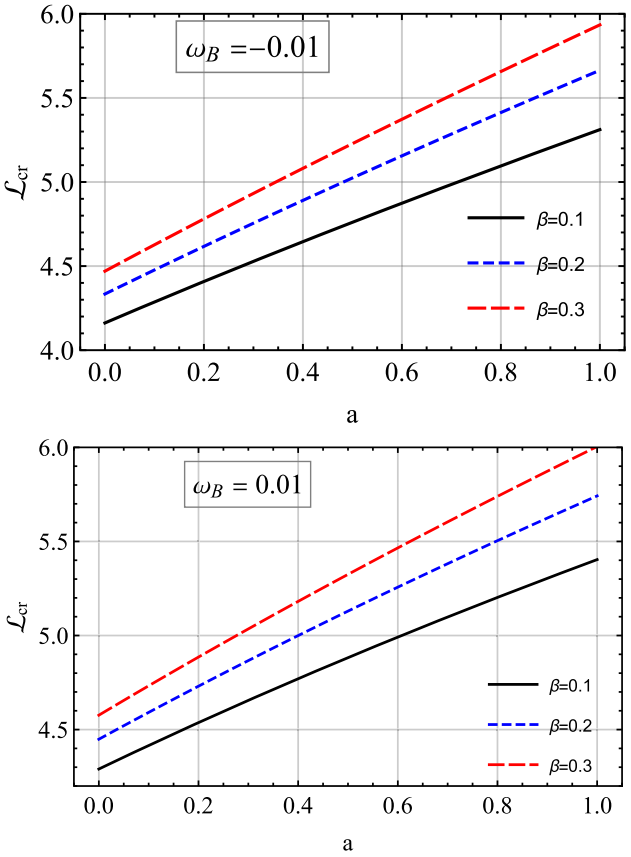

Fig. 9 Graphical behavior of the angular momentum's critical value vs. black hole spin a

Which is in the dimensionless form simplifies to

$$\mathcal{E}^2_{cm}=E^2_{cm}/(2m^2)=1-g_{\mu\nu}u^{\mu}_1u^{\nu}_2. \tag{18}$$

4.2.1 Neutral and electrically charged particles

We will initially look at the collisions between neutral and electrically charged particles. The aforementioned Eqs. (9)–(12) (equations of motion), simplifies the case of neutral particles with the substitution of $\beta=\omega=0$.

Figure 10 depicts the axial dependency of the center of mass energy in the cases of neutral with neutral and electrically charged particles' collision. Our graphical analysis shows that the center of mass energy decreases along the radial profile in both neutral and electrically charged particle collisions, but after some extent, in both cases, the energy increases with increasing values of $|\omega_2|$. Furthermore, $\omega<0$ has a greater impact on the energy release rate compared to $\omega>0$. In short, the electrically charged particles contribute to the center of mass energy.

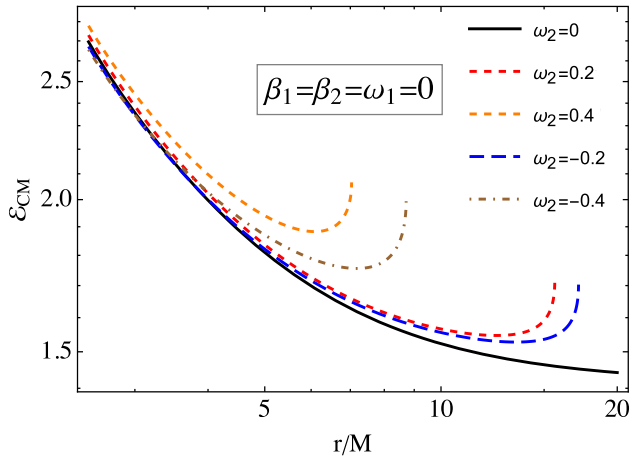

Fig. 10 Axial dependency of the center of mass energy in the case of neutral with electrically charged particle's collision along the radial distance r

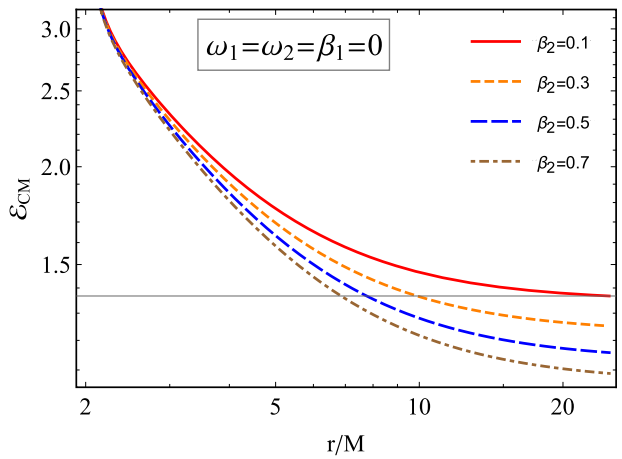

Fig. 11 Axial dependency of the center of mass energy in the case of electrically neutral with magnetized particle collisions

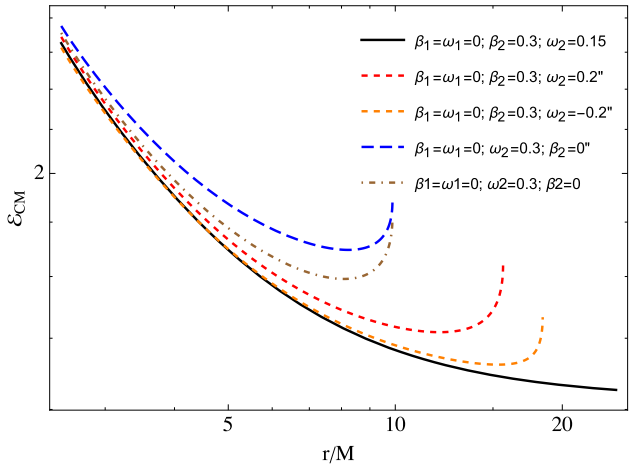

Fig. 12 Axial dependency of the center of mass energy in the case of neutral, electrically charged, and magnetized particle collisions

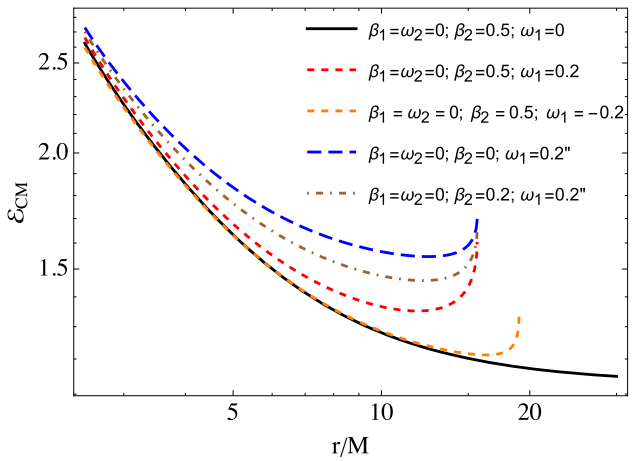

Fig. 13 The radial dependency of the center of mass energy in the collisions of electrically charged and magnetized particles

4.2.2 *Electrically neutral and magnetized particles*

Here, in the second case, we consider collisions of electrically neural and magnetic particles.

In Fig. 11, we investigated the graphical behavior of the energy release rate in the case of electrically neutral particles with a collision of magnetized particles. Our results demonstrate that both ω_2 and the magnetic interaction parameter β_2 greatly influence the energy release rate. In conclusion, ω_2 contributes, while $\beta_2 > 0$ decreases the center of mass energy along the radial profile r.

4.2.3 *Neutral, electrically charged and magnetized particles*

In this subsection, we consider the collisions between neutral and electrically charged and magnetized particles.

In Fig. 12, we examine the center of mass energy's graphical behavior in the collisions between neutral and electrically charged and magnetized particles. Here, we observed that the Larmor parameter ω_2 contributes to the energy release rate. On the other hand, β_2 acts inversely as it diminishes the center of mass energy along the radial profile r.

4.2.4 *Electrically charged and magnetized particles*

This subsection of our article aims to explore the behavior of the center of mass energy in the collisions of electrically charged and magnetized particles.

The graphical behavior in Fig. 13 is shown for various combinations of ω_1 and β_2. Our result demonstrates interesting behavior as $\omega_1 > 0$ contributes, while $\omega_1 < 0$ and β_2 decreases the energy release rate along the radial profile r. In addition, we noted that the collision of neutral and

electrically charged particles has more energy release rate as compared to the other cases of particle collisions.

4.2.5 Electrically charged and electrically charged magnetized particles

The case of electrically charged and electrically charged magnetized particle collisions is plotted in Fig. 14. From our graphical analysis, one can see that β_2 diminishes, the center of mass energy along the radial profile r.

4.2.6 Two magnetized particles

Here, we consider the collision between two magnetized particles only (Fig. 15).

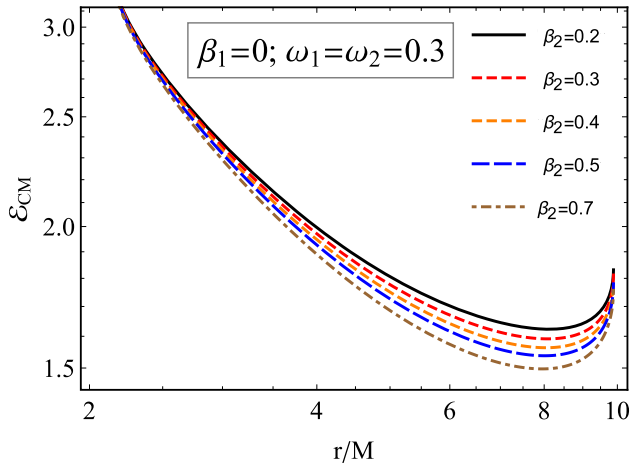

Fig. 14 The radial dependency of the center of mass energy in the collisions of electrically charged and electrically charged magnetized particles

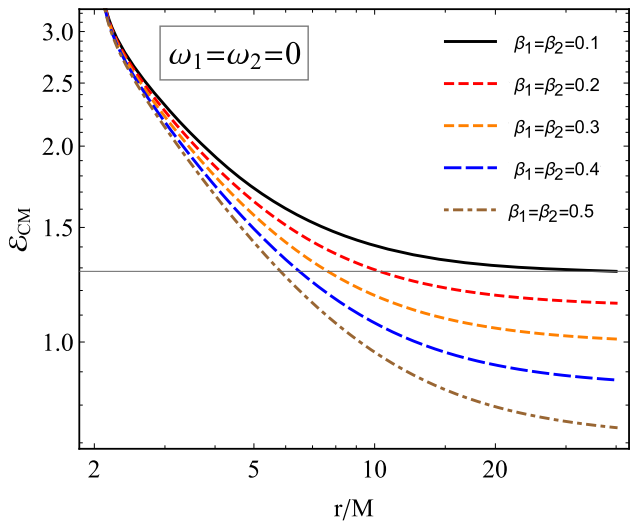

Fig. 15 The radial dependency of the center of mass energy in the collisions of two magnetized particles

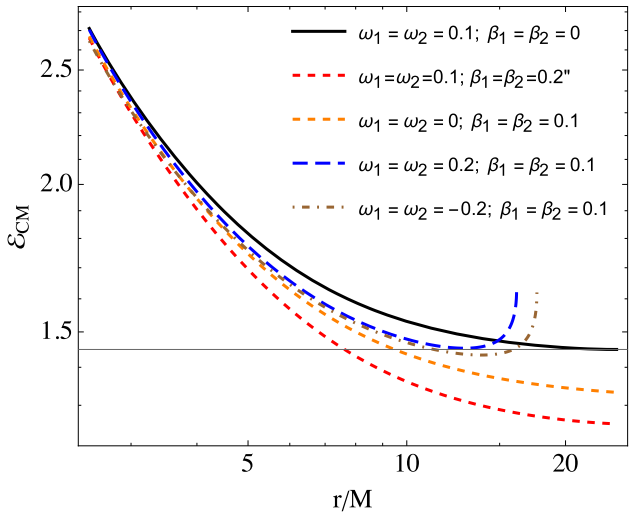

Fig. 16 The radial dependency of the center of mass energy in the collisions of two electrically charged and magnetized particles

From the graphical descriptions, we can see that just like in the previous case the magnetic field influences the energy release rate in the same way, as it diminishes the energy release rate.

4.2.7 Two electrically charged and magnetized particles

In the present subsection, we assumed the collisions of two electrically charged and magnetized particles.

In this case, we have plotted the behavior of the center of mass energy in Fig. 16 at various combinations of the electric and magnetic parameters values. Similarly to the previous case, here in the collisions of two electrically charged and magnetized particles, we observe a decrease in the center of mass energy for the magnetic field. In contrast, one can get more energy for the case of $\omega_1 = \omega_2 > 0$ in comparison with $\omega_1 = \omega_2 < 0$. Moreover, charged particle collision releases much more energy compared to the magnetized particle case near the horizon.

4.2.8 Magnetized, electrically charged and magnetized particles

This subsection of our article aims to explore the behavior of the center of mass energy in collisions of magnetized particles with electrically charged and magnetized particles (Fig. 17).

Our graphical results of the collisions of magnetized particles with electrically charged and magnetized particles show that just like in the previous case the magnetic field decreases the energy release rate. But here the impact of the magnetic field is much higher in comparison with previous cases.

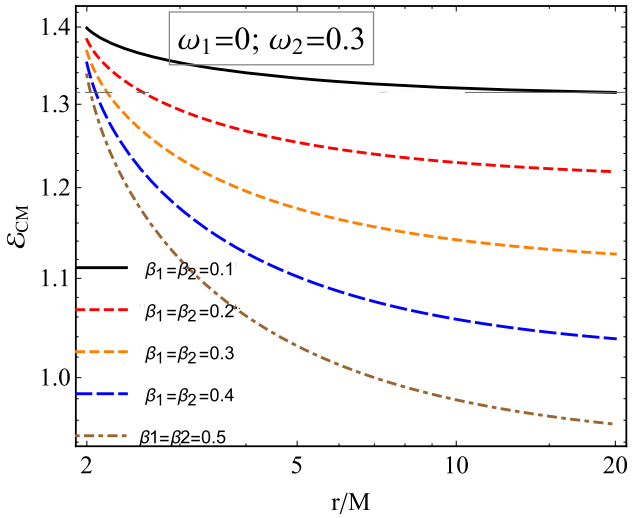

Fig. 17 The radial dependency of the center of mass energy in the collisions of a magnetized particle with electrically charged and magnetized particles

5 Conclusion

Throughout this work, we have investigated the circular motion of test particles carrying electric charge and magnetic dipole moments around magnetized (uncharged) Kerr black holes. First, we have derived the effective potential for the circular motion of the particles, taking into account magnetic interaction with an electrically charged and magnetic dipole moment. We have analyzed the effective potential, angular momentum, and energy of the particles for various values of ω_B and β, which correspond to the interactions of external magnetic fields with the electric charge and magnetic moment of the particles. It is observed that Lorentz forces are proportional to ω_B and are stronger than the magnetic dipole interaction forces. Our main findings are listed below:

- In the case of fasting rotating magnetized Kerr black holes, the ISCO radius is smaller compared to the case of slowly rotating and Schwarzschild-MOG black holes. Moreover, β increases, whereas the black hole spin and ω_B decrease the ISCO radius. Also, we have found that there are contour-like degeneracy values in ω_B and β that provide the same ISCO radius.
- At a particular value of ω_B, the ISCO radius remains unaffected by the magnetic coupling parameter β, providing (almost) the same values of ISCO radius.
- The ISCO energy of the particles increases with an increase of ω_B; however, β and $\omega_B < 0$ decrease it.
- We observed that black hole spin a increases the process of energy extraction. The parameters ω_B and β considerably affect the efficiency of the energy extraction process. As a result, one can extract much more energy in the case of $\beta \neq 0$ compared to $\beta = 0$, whereas $\omega_B < 0$ contributes to the energy extraction while $\omega_B > 0$ decreases it.

Further, we have focused on exploring the collisions of test electrically charged, magnetized, and neutral particles within the metric of magnetized rotating Kerr black holes. To happen the collisions in circular orbits, the radial velocity and its first derivative with respect to r must vanish with corresponding critical angular momentum.

Our numerical and graphical analyses have shown that $\omega > 0$ contributes, whereas $\omega < 0$ decreases the critical value of angular momentum. On the other hand, both spin a and the magnetic coupling parameter β contribute to $\mathcal{L}_{cr}$. Finally, we have investigated the collisions between electrically neutral, magnetized, and electrically charged particles having a dipole magnetic moment by assuming the masses of the colliding particles are the same. We have studied various scenarios of the collisions and obtained the following results:

- In the collisions between neutral and electrically charged and magnetized particles, we have obtained that $\omega_B > 0$ contributes to the energy release rate, while β acts inversely as it diminishes the center of mass energy.
- In the collisions between neutral and electrically charged and magnetized particles, we observed that ω_2 contributes to the energy release rate; however, β_2 acts inversely as it diminishes the center of mass energy.
- For various combinations of ω_1 and β_2 values: our results have shown interesting behavior as $\omega_1 > 0$ contributes, whereas $\omega_1 < 0$ and $\beta_2 > 0$ decreases the energy.
- In the case of electrically charged and electrically charged magnetized particle collisions, we have obtained that the magnetic field diminishes the energy release rate.
- In the absence of electric charge ($\omega_1 = \omega_2 = 0$), just like in the previous cases the positive magnetized particles diminish the center of mass energy.
- In the collisions of electrically charged with electrically charged and magnetized particles, we have obtained a decrease in the center of mass energy for $\beta_2 > 0$.
- The collisions between two electrically charged and magnetized particles: magnetic field diminish the energy release rate. In contrast, we get more energy in the case of $\omega_1 = \omega_2 > 0$ in comparison with $\omega_1 = \omega_2 < 0$. Moreover, charged particle collision releases much more energy compared to the magnetized particle case near the horizon.

Acknowledgements J.R., A.A., and A.B. acknowledge Grant No. FA-F-2021-510 of the Uzbekistan Agency for Innovative Development and J.R. thanks Silesian University in Opava for hospitality.

Data availability This manuscript has no associated data or the data will not be deposited. [Authors' comment: This paper has pure theoretical behavior.]

Code availability Code/software will be made available on reasonable request. [Authors' comment: This paper is a theoretical study and no associated code/software is involved.]

Funded by SCOAP[3].

References

1. A.M. Beloborodov, Astrophys. J. Lett. **566**, L85 (2002). https://doi.org/10.1086/339511
2. S.U. Khan, J. Ren, Chin. J. Phys. **70**, 55 (2021). https://doi.org/10.1016/j.cjph.2020.08.027
3. R.M. Wald, Phys. Rev. D **10**, 1680 (1974). https://doi.org/10.1103/PhysRevD.10.1680
4. J.A. Petterson, Phys. Rev. D **10**, 3166 (1974). https://doi.org/10.1103/PhysRevD.10.3166
5. R.D. Blandford, R.L. Znajek, Mon. Not. R. Astron. Soc. **179**, 433 (1977)
6. A. Tchekhovskoy, in *The Formation and Disruption of Black Hole Jets, Astrophysics and Space Science Library*, ed. by I. Contopoulos, D. Gabuzda, N. Kylafis, vol. 414, p. 45 (2015). https://doi.org/10.1007/978-3-319-10356-3_3
7. P. Goldreich, W.H. Julian, Astrophys. J. **157**, 869 (1969). https://doi.org/10.1086/150119
8. J. Rayimbaev, S. Jumaniyozov, M. Umaraliyev, A. Abdujabbarov, Universe **8**(10), 496 (2022). https://doi.org/10.3390/universe8100496
9. A.A. Abdujabbarov, B.J. Ahmedov, V.G. Kagramanova, Gen. Relativ. Gravit. **40**, 2515 (2008). https://doi.org/10.1007/s10714-008-0635-3
10. Z. Stuchlík, M. Kološ, Eur. Phys. J. C **76**(1), 32 (2016). https://doi.org/10.1140/epjc/s10052-015-3862-2
11. J. Vrba, A. Abdujabbarov, M. Kološ, B. Ahmedov, Z. Stuchlík, J. Rayimbaev, Phys. Rev. D **101**(12), 124039 (2020). https://doi.org/10.1103/PhysRevD.101.124039
12. S. Murodov, K. Badalov, J. Rayimbaev, B. Ahmedov, Z. Stuchlík, Symmetry **16**(1), 109 (2024). https://doi.org/10.3390/sym16010109
13. J. Rayimbaev, N. Juraeva, M. Khudoyberdiyeva, A. Abdujabbarov, M. Abdullaev, Galaxies **11**(6), 113 (2023). https://doi.org/10.3390/galaxies11060113
14. A. Abdujabbarov, J. Rayimbaev, F. Atamurotov, B. Ahmedov, Galaxies **8**(4), 76 (2020). https://doi.org/10.3390/galaxies8040076
15. J. Rayimbaev, D. Bardiev, F. Abdulxamidov, A. Abdujabbarov, B. Ahmedov, Universe **8**(10), 549 (2022). https://doi.org/10.3390/universe8100549
16. S.U. Khan, Z.M. Chen, Eur. Phys. J. C **83**(8), 704 (2023). https://doi.org/10.1140/epjc/s10052-023-11897-x. [Erratum: Eur. Phys. J. C **83**, 760 (2023)]
17. A.N. Aliev, D.V. Galtsov, Sov. Phys. Usp. **32**, 75 (1989). https://doi.org/10.1070/PU1989v032n01ABEH002677
18. A.N. Aliev, N. Ozdemir, Mon. Not. R. Astron. Soc. **336**, 241 (2002). https://doi.org/10.1046/j.1365-8711.2002.05727.x
19. S.S. Komissarov, Mon. Not. R. Astron. Soc. **350**, 407 (2004). https://doi.org/10.1111/j.1365-2966.2004.07446.x
20. J.R. Rayimbaev, Astrophys. Space Sci. **361**, 288 (2016). https://doi.org/10.1007/s10509-016-2879-9
21. B. Narzilloev, J. Rayimbaev, A. Abdujabbarov, C. Bambi, Eur. Phys. J. C **80**(11), 1074 (2020). https://doi.org/10.1140/epjc/s10052-020-08623-2
22. M. Zahid, J. Rayimbaev, S.U. Khan, J. Ren, S. Ahmedov, I. Ibragimov, Eur. Phys. J. C **82**(5), 494 (2022). https://doi.org/10.1140/epjc/s10052-022-10432-8
23. S. Ullah Khan, J. Rayimbaev, Z.M. Chen, Z. Stuchlík, (2023). arXiv:2311.16936
24. D. Kunneriath, G. Witzel, A. Eckart, M. Zamaninasab, R. Gießübel, R. Schödel, F.K. Baganoff, M.R. Morris, M. Dovčiak, W.J. Duschl, M. García-Marín, V. Karas, S. König, T.P. Krichbaum, M. Krips, R.S. Lu, J. Mauerhan, J. Moultaka, K. Mužić, N. Sabha, F. Najarro, J.U. Pott, K.F. Schuster, L.O. Sjouwerman, C. Straubmeier, C. Thum, S.N. Vogel, P. Teuben, A. Weiss, H. Wiesemeyer, J.A. Zensus, Astron. Astrophys. **517**, A46 (2010). https://doi.org/10.1051/0004-6361/200913613
25. A. Eckart, M. García-Marín, S.N. Vogel, P. Teuben, M.R. Morris, F. Baganoff, J. Dexter, R. Schödel, G. Witzel, M. Valencia-S., V. Karas, D. Kunneriath, C. Straubmeier, L. Moser, N. Sabha, R. Buchholz, M. Zamaninasab, K. Mužić, J. Moultaka, J.A. Zensus, Astron. Astrphys **537**, A52 (2012). https://doi.org/10.1051/0004-6361/201117779
26. R.P. Eatough, H. Falcke, R. Karuppusamy, K.J. Lee, D.J. Champion, E.F. Keane, G. Desvignes, D.H.F.M. Schnitzeler, L.G. Spitler, M. Kramer, B. Klein, C. Bassa, G.C. Bower, A. Brunthaler, I. Cognard, A.T. Deller, P.B. Demorest, P.C.C. Freire, A. Kraus, A.G. Lyne, A. Noutsos, B. Stappers, N. Wex, Nature **501**(7467), 391 (2013). https://doi.org/10.1038/nature12499
27. M. Nakamura, K. Asada, K. Hada, H.Y. Pu, S. Noble, C. Tseng, K. Toma, M. Kino, H. Nagai, K. Takahashi, J.C. Algaba, M. Orienti, K. Akiyama, A. Doi, G. Giovannini, M. Giroletti, M. Honma, S. Koyama, R. Lico, K. Niinuma, F. Tazaki, Atsophys. J. **868**(2), 146 (2018). https://doi.org/10.3847/1538-4357/aaeb2d
28. R. Penrose, Nuovo Cimento Rivista Serie **1**, 252 (1969)
29. T. Piran, J. Shaham, J. Katz, Astrophys. J. Lett. **196**, L107 (1975)
30. T. Piran, J. Shaham, Phys. Rev. D **16**, 1615 (1977). https://doi.org/10.1103/PhysRevD.16.1615
31. M. Banados, J. Silk, S.M. West, Phys. Rev. Lett. **103**, 111102 (2009). https://doi.org/10.1103/PhysRevLett.103.111102
32. M. Zahid, S.U. Khan, J. Ren, Chin. J. Phys. **72**, 575 (2021). https://doi.org/10.1016/j.cjph.2021.05.003
33. M. Zahid, S.U. Khan, J. Ren, J. Rayimbaev, Int. J. Mod. Phys. D **31**(08), 2250058 (2022). https://doi.org/10.1142/S0218271822500584
34. M. Banados, B. Hassanain, J. Silk, S.M. West, Phys. Rev. D **83**, 023004 (2011). https://doi.org/10.1103/PhysRevD.83.023004
35. T. Harada, M. Kimura, Phys. Rev. D **83**, 084041 (2011). https://doi.org/10.1103/PhysRevD.83.084041
36. M. Kimura, K.I. Nakao, H. Tagoshi, Phys. Rev. D **83**, 044013 (2011). https://doi.org/10.1103/PhysRevD.83.044013
37. E. Berti, R. Brito, V. Cardoso, Phys. Rev. Lett. **114**(25), 251103 (2015). https://doi.org/10.1103/PhysRevLett.114.251103
38. M. Shahzadi, Z. Yousaf, S.U. Khan, Phys. Dark Univ. **24**, 100263 (2019). https://doi.org/10.1016/j.dark.2019.100263

39. K. Haydarov, J. Rayimbaev, A. Abdujabbarov, S. Palvanov, D. Begmatova, Eur. Phys. J. C **80**(5), 399 (2020). https://doi.org/10.1140/epjc/s10052-020-7992-9
40. E. Berti, V. Cardoso, L. Gualtieri, F. Pretorius, U. Sperhake, Phys. Rev. Lett. **103**, 239001 (2009). https://doi.org/10.1103/PhysRevLett.103.239001
41. T. Jacobson, T.P. Sotiriou, Phys. Rev. Lett. **104**, 021101 (2010). https://doi.org/10.1103/PhysRevLett.104.021101
42. V.P. Frolov, Phys. Rev. D **85**, 024020 (2012). https://doi.org/10.1103/PhysRevD.85.024020
43. S. Murodov, J. Rayimbaev, B. Ahmedov, A. Hakimov, Symmetry **15**(11), 2084 (2023). https://doi.org/10.3390/sym15112084
44. J. Rayimbaev, S. Shaymatov, F. Abdulxamidov, S. Ahmedov, D. Begmatova, Universe **9**(3), 135 (2023). https://doi.org/10.3390/universe9030135
45. V.P. Frolov, A.A. Shoom, Phys. Rev. D **82**(8), 084034 (2010). https://doi.org/10.1103/PhysRevD.82.084034
46. A. Tursunov, Z. Stuchlík, M. Kološ, Phys. Rev. D **93**(8), 084012 (2016). https://doi.org/10.1103/PhysRevD.93.084012
47. G. Preti, Phys. Rev. D **70**(2), 024012 (2004). https://doi.org/10.1103/PhysRevD.70.024012
48. C.W. Misner, K.S. Thorne, J.A. Wheeler, *Gravitation* (W. H. Freeman, San Francisco, 1973)
49. J. Bicak, Z. Stuchlik, V. Balek, Bull. Astron. Inst. Czechoslovakia **40**, 65 (1989)
50. I.D. Novikov, K.S. Thorne, in *Black Holes (Les Astres Occlus)* (1973), pp. 343–450
51. W.H. Bian, Y.H. Zhao, Publ. Astron. Soc. Jpn. **55**, 599 (2003). https://doi.org/10.1093/pasj/55.3.599
52. S.M. Wagh, S.V. Dhurandhar, N. Dadhich, Astrophys. J. **290**, 12 (1985). https://doi.org/10.1086/162952
53. A.A. Abdujabbarov, B.J. Ahmedov, S.R. Shaymatov, A.S. Rakhmatov, Astrophys. Space Sci. **334**, 237 (2011). https://doi.org/10.1007/s10509-011-0740-8
54. N. Dadhich, A. Tursunov, B. Ahmedov, Z. Stuchlík, Mon. Not. R. Astron. Soc. **478**(1), L89 (2018). https://doi.org/10.1093/mnrasl/sly073
55. M. Bañados, J. Silk, S.M. West, Phys. Rev. Lett. **103**(11), 111102 (2009). https://doi.org/10.1103/PhysRevLett.103.111102
56. M. Bañados, B. Hassanain, J. Silk, S.M. West, Phys. Rev. D **83**(2), 023004 (2011). https://doi.org/10.1103/PhysRevD.83.023004
57. T. Harada, M. Kimura, Phys. Rev. D **83**(2), 024002 (2011). https://doi.org/10.1103/PhysRevD.83.024002
58. S.W. Wei, Y.X. Liu, H. Guo, C.E. Fu, Phys. Rev. D **82**(10), 103005 (2010). https://doi.org/10.1103/PhysRevD.82.103005
59. O.B. Zaslavskii, Phys. Rev. D **82**(8), 083004 (2010). https://doi.org/10.1103/PhysRevD.82.083004
60. O.B. Zaslavskii, Sov. J. Exp. Theor. Phys. Lett. **92**, 571 (2011). https://doi.org/10.1134/S0021364010210010
61. O.B. Zaslavskii, Class. Quantum Gravity **28**(10), 105010 (2011). https://doi.org/10.1088/0264-9381/28/10/105010
62. M. Kimura, K.I. Nakao, H. Tagoshi, Phys. Rev. D **83**(4), 044013 (2011). https://doi.org/10.1103/PhysRevD.83.044013
63. T. Igata, T. Harada, M. Kimura, Phys. Rev. D **85**(10), 104028 (2012). https://doi.org/10.1103/PhysRevD.85.104028
64. V.P. Frolov, Phys. Rev. D **85**(2), 024020 (2012). https://doi.org/10.1103/PhysRevD.85.024020
65. F. Atamurotov, B. Ahmedov, S. Shaymatov, Astrophys. Space Sci. **347**, 277 (2013). https://doi.org/10.1007/s10509-013-1527-x
66. C. Liu, S. Chen, C. Ding, J. Jing, Phys. Lett. B **701**, 285 (2011). https://doi.org/10.1016/j.physletb.2011.05.070
67. N. Juraeva, J. Rayimbaev, A. Abdujabbarov, B. Ahmedov, S. Palvanov, Eur. Phys. J. C **81**, 124078 (2021). https://doi.org/10.1140/epjc/s10052-021-08876-5
68. A. Tursunov, M. Kološ, A. Abdujabbarov, B. Ahmedov, Z. Stuchlík, Phys. Rev. D **88**(12), 124001 (2013). https://doi.org/10.1103/PhysRevD.88.124001
69. Z. Stuchlík, S. Hledík, K. Truparová, Class. Quantum Gravity **28**(15), 155017 (2011). https://doi.org/10.1088/0264-9381/28/15/155017
70. S.U. Khan, M. Shahzadi, J. Ren, Phys. Dark Univ. **26**, 100331 (2019). https://doi.org/10.1016/j.dark.2019.100331
71. A. Abdujabbarov, J. Rayimbaev, F. Atamurotov, B. Ahmedov, Galaxies **8**(4), 76 (2020). https://doi.org/10.3390/galaxies8040076